CALCULATION OF DISPERSION CURVES IN BONDED JOINTS USING EITHER COMPLEX FREQUENCY OR COMPLEX SLOWNESS AND COMPARISON OF THE RESULTS WITH THE MINIMA OF THE PLANE WAVE REFLECTION COEFFICIENTS

A. Bernard and M. Lowe
Department of Mechanical Engineering
Imperial College of Science and Technology and Medicine,
London SW7 2BX
UK

M. Deschamps
Laboratoire de Mécanique Physique
Université Bordeaux I, URA C.N.R.S no 867.
33405 Talence Cedex
France

INTRODUCTION

Oblique incidence methods using ultrasonic waves are often proposed for the inspection of multilayered plates. For example, during the bonding process between two plates of titanium, the possibility of the formation of a brittle layer of "Alpha case" (or "Hard Alpha") along the bondline has been established if nitrogen or oxygen is present [1]. Moreover, adhesive joints, which are widely used in industry, need to be inspected in order to confirm the properties of the adhesive layer (cohesion) and of its interfaces with the adherends (adhesion). One possible technique for inspection is to exploit the properties of guided waves which travel along the embedded layer. According to the coincidence angle principle, they can be excited by signals incident at a precise angle and there is an expectation that the generation of a plate mode is indicated by a minimum of the plane wave reflection coefficient. As plate modes are very sensitive to the properties of the embedded layer in which they travel, the waves which are excited within the adherent (adhesive joint) or within the bondline (diffusion bonded joint) would therefore give information on their properties [2]. This method of excitation and detection is practically valid in many circumstances such as immersed plates in water [3] as shown in Figure 1. However, when the surrounding medium has an impedance of similar order to the layer, minima of the reflection coefficient do not indicate the generation of guided modes in the layer [4-6].

This difference prompted the authors to investigate another approach to the problem. Instead of solving in real frequency and complex slowness (as is conventional for leaky waves),

Review of Progress in Quantitative Nondestructive Evaluation, Vol 17
Edited by D.O. Thompson and D.E. Chimenti, Plenum Press, New York, 1998

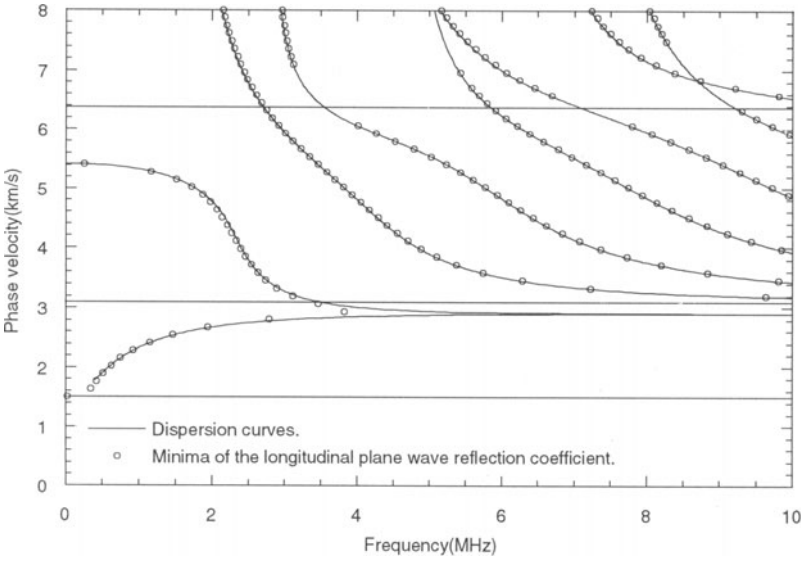

Figure 1. Comparison between the minima of the longitudinal plane wave reflection coefficient and the dispersion curves calculated in real frequency and complex slowness for 1 mm thick Aluminium plate immersed in water.

the solution is found in complex frequency and real slowness as already introduced by Poncelet and Deschamps for immersed isotropic [7] or anisotropic [8] plates. In their papers, the differences introduced by the imaginary part in the frequency are analysed and the necessity to consider the notion of slowness and the notion of frequency, instead of simply wave number, which contains both the time and the spatial information, is explained. They also show the differences due to the introduction of the complex frequency in the calculation of the dispersion curves and compare them to the usual leaky Lamb wave dispersion curves. Finally they consider the effect of the fluid density. Their work identifies a difference between spatial and temporal decay of the wave amplitude. Because the amplitudes of leaky waves decay as they travel, the concept of spatial attenuation has been conventionally adopted in the literature. It is commonly modelled by a complex wave number which is described by a real frequency and a complex slowness. However transient phenomena can sometimes be observed and then an attenuation in time has to be introduced. This is done by assuming the frequency to be complex. Therefore, the notion of complex frequency and real slowness models an attenuation due only to the time but not to the space. The modal solutions of the complex frequency formulation are fundamentally different from the conventional complex slowness solutions; they do not simply represent a change in variables when solving the modal problem.

We show here for a solid layer embedded in another solid that the dispersion curves calculated in complex frequency are again very different from the curves calculated in complex slowness. Moreover, the dispersion curves for complex frequency present very much better agreement with the minima of the plane wave reflection coefficients than the conventional curves. The paper will discuss the nature of these findings which have general relevance to the development of NDE techniques.

THEORY

In an infinite isotropic solid, two different types of waves, satisfying the equation of motion may exist: one describing longitudinal plane waves (L) and the other describing shear plane waves (T). Both have the form:

$$\vec{u}^{\pm}_{L,T} = \mathrm{Re}\left\{ {}^{*}\xi^{\pm}_{L,T}\, {}^{*}\vec{P}\, e^{i({}^{*}\omega t - {}^{*}\vec{K}.\vec{M})} \right\} \qquad (1)$$

where: ${}^{*}\xi$ is the complex amplitude (+ for the waves travelling towards the positive y direction which is normal to the interface, - otherwise) and ${}^{*}\vec{P} = \vec{P}' - i\vec{P}''$ represents the unit length polarisation vector (${}^{*}\vec{P}.{}^{*}\vec{P} = 1$). Because the polarisation is complex, the displacements are described by ellipses whose major and minor axes are defined respectively by $\vec{P}'$ and $\vec{P}''$, the imaginary part of the amplitude representing therefore the position of the displacement vector in the base ($\vec{P}', \vec{P}''$). Moreover, ${}^{*}\vec{K} = \vec{K}' - i\vec{K}'' = {}^{*}\omega\, {}^{*}\vec{S}$ stands for the complex wave number, ${}^{*}\omega = \omega' + i\omega''$ is the complex angular frequency, ${}^{*}\vec{S} = \vec{S}' - i\vec{S}''$ is the complex slowness and $\vec{M}$ the position vector. The notation Re{} denotes the real part and the superscript indices * on the left hand side indicate that the quantities are complex. The propagation vector is denoted $\vec{K}'$ and the attenuation vector is represented by $\vec{K}''$. The real positive scalar ω' stands for the angular frequency. The parameter ω'' is the extinction coefficient ($\omega'' > 0$) or the switching-on coefficient ($\omega'' < 0$) of the source. After expansion of this displacement one can show that the phase velocity can be written in the most general case as:

$$Vph = \frac{\omega'}{\omega' S' + \omega'' S''} \qquad (2)$$

Since attenuation in both time and space may be considered, it is necessary to distinguish between phenomena due to time and space. The terms slowness (inverse of the velocity) and frequency will be preferred to the term wave number, which contains both space and time components (${}^{*}\vec{K} = {}^{*}\omega\, {}^{*}\vec{S}$), to describe the properties of the waves. From an experimental point of view, the hypothesis of real slowness will best be satisfied if very large transducers are used such that the assumption of an infinite plane wave is well approached. Together with this, the hypothesis of complex frequency requires a discontinuity in time in the excitation signal.

Thus, two extreme kinds of problems can be considered: either the spatial effects are predominant and the frequency is real and the slowness is complex, or the time effects are predominant and the frequency is complex and the slowness is real. Accordingly, an infinity of other problems can therefore be examined with both the frequency and the slowness complex.

REFLECTION PROBLEM

The geometry which is studied is presented in Figure 2 where the incident wave can either be a longitudinal or a shear infinite homogeneous plane wave. A solid medium (labelled 2) is embedded in two other identical semi-infinite solids (labelled 1). They are purely isotropic and they are considered to be infinite in the x-direction. As the layers are perfectly connected at the interfaces, the continuity of the velocities and of the stresses between the medium 1 and the medium 2 at the two boundaries must be satisfied [9]. This leads to a system of eight equations with eight unknowns which are the amplitudes of the waves. This well known problem can then be written:

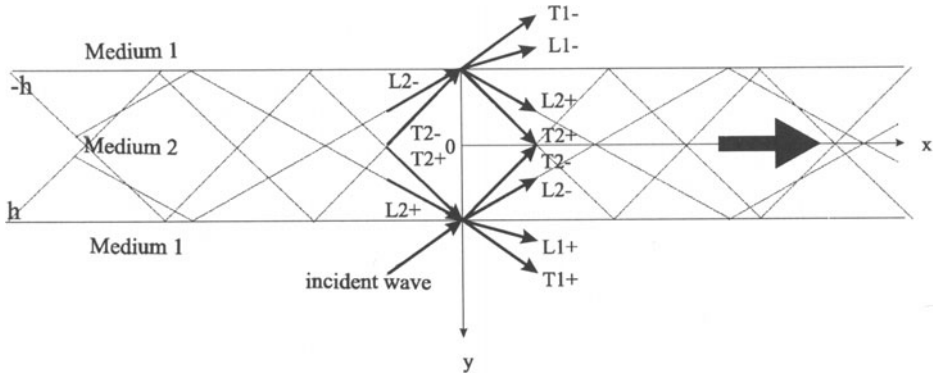

Figure 2. Plate configuration: layer embedded in a solid medium showing partial waves.

$$[[A]]\vec{X} = \begin{bmatrix} -\vec{I} \\ \vec{0} \end{bmatrix} \tag{3}$$

where

$$[[A]] = \begin{bmatrix} \vec{L}_1^+ & \vec{T}_1^+ & -\vec{L}_2^- & -\vec{T}_2^- & 0 & 0 & -\vec{L}_2^+ & -\vec{T}_2^+ \\ 0 & 0 & -\vec{L}_2^- & -\vec{T}_2^- & \vec{L}_1^- & \vec{T}_1^- & -\vec{L}_2^+ & -\vec{T}_2^+ \end{bmatrix} \begin{matrix} \text{at } y = h \\ \text{at } y = -h \end{matrix} \tag{4}$$

and

$$\vec{X} = (\xi_{L1}^+ \quad \xi_{T1}^+ \quad \xi_{L2}^- \quad \xi_{T2}^- \quad \xi_{L1}^- \quad \xi_{T1}^- \quad \xi_{L2}^+ \quad \xi_{T2}^+)^T \tag{5}$$

In the above notation, each vector L and T contains the two displacements and the two stresses characteristic of each wave presented in Figure 2, the subscript numbers standing for the labels of the media. The + defines the waves travelling in the direction of the positive y-axis and the - represents the waves travelling in the direction of the negative y-axis. The vector I stands for the incident wave and the vector X represents the amplitudes of the waves. In the following, the shear plane wave reflection coefficient will be calculated for a shear incident plane wave and the longitudinal plane wave reflection coefficient will be calculated for a longitudinal incident plane wave. Thus, the longitudinal plane wave reflection coefficient is defined by the ratio between the amplitude of the longitudinal reflected signal (L1+) and the amplitude of the longitudinal incident signal, and the shear plane wave reflection coefficient is defined by the ratio between the amplitude of the shear reflected signal (T1+) and the amplitude of the shear incident signal.

MODAL PROBLEM

The definition of the modal problem is given by Figure 2 without any incident wave [9]. The system is unforced and the waves are supposed to be able to propagate without input of energy: equation (3) where the vector I is null. This equation is satisfied when det(A)=0. Thus, we look for the solutions of a function F such that $F(^*\omega, ^*S)=0$. The solutions of this transcendental equation, which usually requires a numerical algorithm to be solved, are the dispersion curves. For the calculation in complex frequency and real slowness we use a Newton-Raphson algorithm providing fast computation. The dispersion curves for the conventional

assumption of real frequency and complex slowness are calculated using a general purpose model developed by Lowe [9] and Pavlakovic et al [10].

RESULTS AND DISCUSSION

As already mentioned in the introduction, a number of multilayered geometries are of interest for non-destructive evaluation. We decided in this paper to present the case of the diffusion bonded joint (0.1 mm thick layer of Alpha Case embedded in titanium), the adhesive joint being still under investigation. The bulk velocities of Alpha case have been measured to be about 5 to 10 % faster than those of titanium but its density is roughly the same [11]. The elastic properties which are used here for the titanium and the Alpha case are respectively: C_{L1}=6.06 km/s, C_{T1}=3.23 km/s, ρ_1=4.46 T/m^3, C_{L2}=6.66 km/s, C_{T2}=3.553 km/s and ρ_2=4.46 T/m^3. This configuration therefore comprises two materials which have roughly the same impedance, the embedded layer being slightly stiffer than the embedding one.

Let us first examine the comparison between the minima of the shear (empty circles for a shear incident plane wave) and the longitudinal (filled circles for a longitudinal incident plane wave) plane wave reflection coefficients with the classical dispersion curves (lines) calculated in real frequency and complex slowness presented in Figure 3 (from [5]). First of all, we have to say that because of their very high attenuation, leading to solutions which are not physically useful, the modes have not been traced over the full solution space. As presented in Figure 3, there is no region, in this frequency range, where the minima of the reflection coefficients coincide with the dispersion curves, although the leaky shear modes and the minima seem to correlate better as the frequency increases. The convergence of the minima towards the modes at high frequency is also accompanied by a reduction in attenuation (values given in reference [6]) and led Lowe and Cawley to suggest that the separation of minima and modes is related to the rate of leakage. It is clear therefore that the measurement of minima of the reflection coefficients do not reveal the (conventional) harmonic heterogeneous modal properties. For the same configuration, let us now compare the minima of both the shear and the longitudinal plane wave reflection coefficients and the dispersion curves calculated in complex frequency and real slowness (Figure 4). It is interesting to note that in the region where excellent agreement between the complex frequency dispersion curves and the minima of the plane wave reflection coefficient is obtained (below the longitudinal bulk velocity of the titanium C_{L1}), the minima of the shear plane wave reflection coefficient are true zeroes; above the longitudinal bulk velocity of the titanium the agreement deteriorates progressively as the phase velocity increases and zeroes of the plane wave reflection coefficients can only be obtained by searching in the complex plane (complex frequency or complex slowness).

The zeroes of the shear plane wave reflection coefficient (complex frequency and real slowness) corresponding to the curve labelled "mode 1" on Figure 4 are shown in Figure 5. For different values of the slowness, we find the complex frequency for which the shear plane wave reflection coefficient is zero. Two kinds of curves can be analysed in the figure. Part a) shows a comparison between the dispersion curve and the zeroes of the reflection coefficient and part b) shows the dimensionless factor $\Omega=\omega''/\omega'$ both versus the real part of the frequency. First of all, let us analyse the reflection coefficient zeroes. As presented, the attenuation factor Ω exhibits two different regions. In the first one (path going from D to C and from C to B), its value is zero and this corresponds to the part of the curve which is below C_{L1} in Figure 5a). Suddenly, its magnitude takes a positive value, then drops to finish negative at around 15 MHz and this corresponds to the part of the curve above C_{L1} in Figure 5a) and to the path between A and B. Moreover, it can be seen that the dispersion curve and the zeroes of the shear plane wave reflection coefficient in Figure 5a) are almost exactly equal below the longitudinal bulk

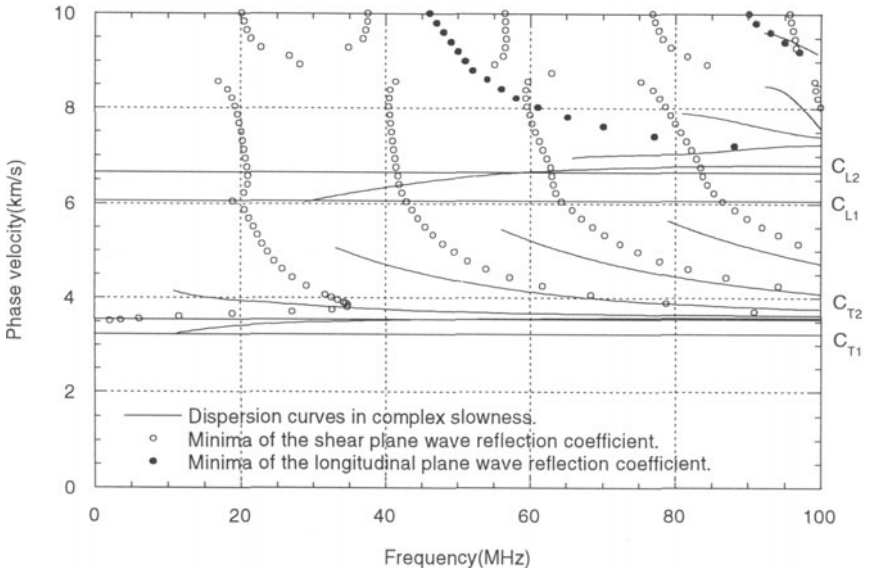

Figure 3. Comparison between the minima of both the shear and the longitudinal plane wave reflection coefficients and the dispersion curves calculated in real frequency and complex slowness for a 0.1 mm thick layer of Hard Alpha embedded in titanium (from [5]).

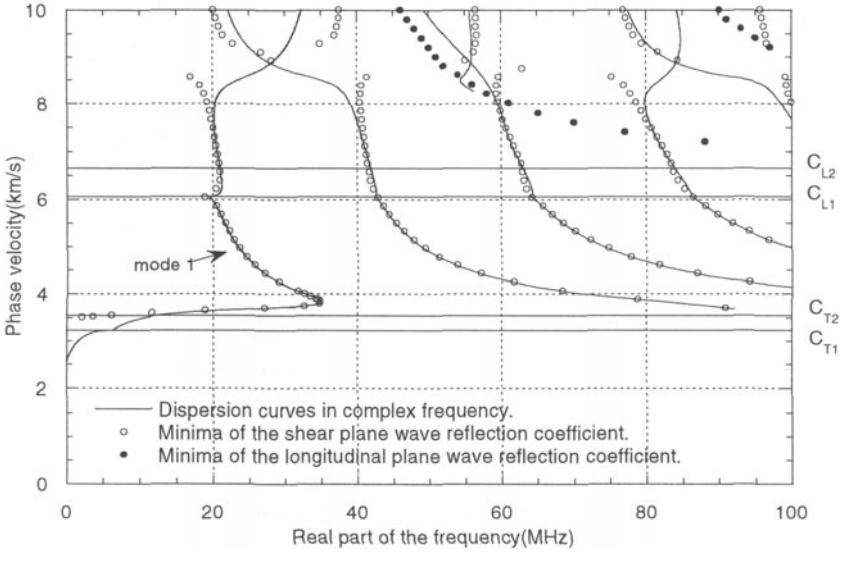

Figure 4. Comparison between the minima of both the shear and the longitudinal plane wave reflection coefficients and the dispersion curves calculated in complex frequency and real slowness for a 0.1 mm thick layer of Hard Alpha embedded in titanium.

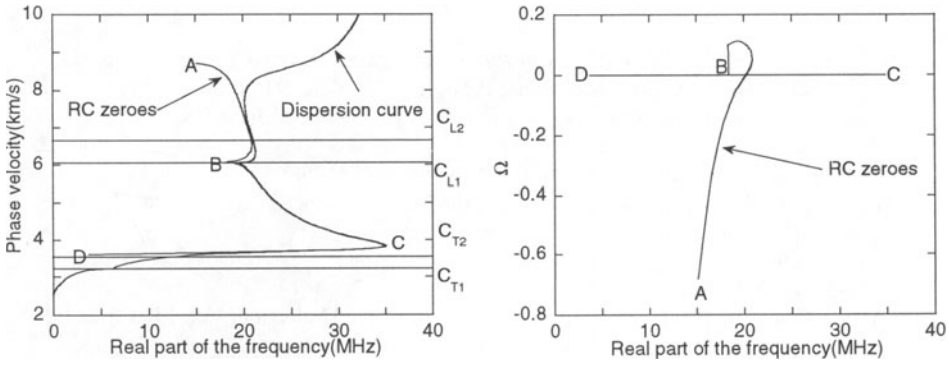

a) Comparison between the zeroes of the reflection coefficient and the dispersion curve.

b) Attenuation factor ($\Omega=\omega''/\omega'$) of zeroes of the complex reflection coefficient.

Figure 5. Comparison between the zeroes of the shear plane wave reflection coefficient and a dispersion curve, both calculated in complex frequency and real slowness.

velocity of the titanium when the zeroes have a null attenuation factor Ω. However, above C_{L1}, the imaginary part of the zeroes becomes significant and the dispersion curve does not correspond to the zeroes anymore. Finally, above 8 km/s, the disagreement is very large and corresponds to the largest magnitudes of Ω. Because these phenomena have been observed for all the modes, we conclude then that the extent of the difference between the zeroes of the reflection coefficients and the dispersion curves calculated in complex frequency corresponds to the magnitude of the imaginary part. The greater the imaginary part of the zeroes of the reflection coefficient, the greater the difference between the curves.

CONCLUSION

The notion of complex frequency has been introduced in order to solve the modal and the response problem differently from the usual procedures which consider the slowness complex and the frequency real. A comparison between the dispersion curves calculated in complex slowness and real frequency, the dispersion curves calculated in complex frequency and real slowness and the zeroes of the longitudinal and shear plane wave reflection coefficients has been presented.

In the case presented, we have shown that the dispersion curves calculated in complex frequency and real slowness can be very different from the dispersion curves calculated in real frequency and complex slowness. This agrees with the fact that these two problems have different physical meanings: the attenuation is either considered in time (complex frequency and real slowness) or in space (real frequency and complex slowness). Moreover one can see better agreement between the dispersion curves, calculated in complex frequency and real slowness, and the zeroes of the plane wave reflection coefficients. The disagreement observed above the longitudinal bulk velocity of the titanium corresponds to the presence of a non-null imaginary part in the zeroes of the reflection coefficient. Work is ongoing to understand the physical nature of these predicted phenomena, in particular why the correlation is better for a computation in complex frequency and real slowness rather than in real frequency and complex slowness.

ACKNOWLEDGEMENT

The authors gratefully acknowledge support from the British Council for their collaboration in this research, via a British Council fellowship for A. Bernard.

REFERENCES

1. M. Lowe and P. Cawley, in *Review of Progress in Quantitative NDE,* Vol. 12, eds. D.O. Thompson and D.E. Chimenti. (Plenum Press, New York, 1993), p. 1653-1659.
2. Y. Bar-Cohen and A.K. Mal, in *Review of Progress in Quantitative NDE,* Vol. 9 , *op.cit* (1992), p. 1271-1277.
3. D. Worlton, Journal of Applied Physics, 32, p. 967-971 (1961).
4. D.E. Chimenti and S.I. Rokhlin, Journal of the Acoustical Society of America, 88, p. 1603-1611 (1990).
5. M. Lowe and P. Cawley, in *Review of Progress in Quantitative NDE,* Vol. 14B, *op.cit.* (1995), p. 1505-1512.
6. M.J.S. Lowe and P. Cawley, Journal of Non-destructive Evaluation, Vol. 13, p. 185-199 (1994).
7. O. Poncelet and M. Deschamps, Journal of the Acoustical Society of America, 102, p. 292-300 (1997).
8. M. Deschamps and O. Poncelet, "Plate waves with complex frequency and total transmission", in proceedings of ultrasonics world congress, Yokohama, 1997, ISBN 4-9900616-0-8 (in press).
9. M. Lowe, IEEE Transactions on Ultrasonics, Ferroelectrics and Frequency control, 42, 525-542 (1995).
10. B. Pavlakovic, *et al.*, in *Review of progress in Quantitative NDE,* Vol. 16, *op.cit.* (1997), p. 185-192.
11. R. Thompson, *et al.*, in *Review of Progress in Quantitative NDE,* Vol. 11, *op.cit.*(1992), p. 1725-1731.